Article:

eprints@whiterose.ac.uk
https://eprints.whiterose.ac.uk/

Filament Behavior in a Computational Model of Ventricular Fibrillation in the Canine Heart

Richard H. Clayton* and Arun V. Holden

Abstract—The aim of this paper was to quantify the behavior of filaments in a computational model of re-entrant ventricular fibrillation. We simulated cardiac activation in an anisotropic monodomain with excitation described by the Fenton–Karma model with Beeler-Reuter restitution, and geometry by the Auckland canine ventricle. We initiated re-entry in the left and right ventricular free walls, as well as the septum. The number of filaments increased during the first 1.5 s before reaching a plateau with a mean value of about 36 in each simulation. Most re-entrant filaments were between 10 and 20 mm long. The proportion of filaments touching the epicardial surface was 65%, but most of these were visible for much less than one period of re-entry. This paper shows that useful information about filament dynamics can be gleaned from models of fibrillation in complex geometries, and suggests that the interplay of filament creation and destruction may offer a target for antifibrillatory therapy.

Index Terms—Cardiac arrhythmia, computational model, fibrillation, re-entry.

I. INTRODUCTION

DURING ventricular fibrillation (VF), electrical activation of the ventricles is rapid, self sustained, and has a complex spatiotemporal pattern. VF results in haemodynamic collapse, and is quickly lethal unless normal rhythm can be restored by a defibrillating shock. Evidence from both experimental [1]–[4] and computational [5]–[7] studies supports the idea that the rapid ventricular activation during VF is sustained by re-entry. During re-entry an action potential continuously propagates into recovered tissue, and rotates around a phase singularity [4] that is a point in two dimensionsand a filament in three dimensions. There is evidence that VF could be sustained by either a single re-entrant wave with fibrillatory conduction [8], or by breakup of an initial reentrant wave to multiple wavelet re-entry. Multiple mechanisms could underlie breakup [9], and these include intrinsic three-dimensional (3-D) instabilities [10], restitution [11], [12], and the effects of rotational anisotropy in the ventricular wall [13].

Although recent developments in experimental technology have enabled imaging of electrical activity within the ventricular wall [14], most experimental studies of re-entry and VF have recorded activity only from a thin layer close to the endocardial, epicardial or transmural (cut) surface of experimental preparations [1], [4], [8], [15], and so can only identify the intersection of a re-entrant wave and its associated filament with the tissue surface. Several techniques for detecting the location and chirality of phase singularities have been developed [4], [16], [17] have been developed, but the 3-D configuration of filaments can only be inferred from them. Using this kind of approach experimental studies have classified only a small proportion of active wavefronts during VF as re-entrant, and have found that the surface manifestation of re-entrant waves persist for only a short time [1], [17]–[19].

Computational models of action potential propagation in cardiac tissue are becoming increasingly sophisticated [20], [21], and have been used to study the 3-D mechanisms that are consistent with measured patterns of surface activation during VF [22], [23]. The output of computational models is data-rich, and can be dissected in space and time to identify features such as filaments.

An earlier computational study using the complex and anatomically detailed geometry of the canine ventricles showed that the number of filaments during simulated VF was dependent on the size of the ventricles [24].

In previous studies we have described a method for identifying filaments and classifying their interaction in a computational model of re-entrant VF in simulated 3-D slabs of tissue [25], [26]. The aim of this study was, therefore, to build on this previous study [24] by extracting detailed information about filament dynamics and their interaction during simulated re-entrant VF in an anatomically detailed model of canine ventricles.

II. METHODS

A. Computational Model of Action Potential Propagation

We described action potential propagation in an anisotropic monodomain using a parabolic reaction diffusion equation

$$C_m \frac{\partial V_m}{\partial t} = \nabla \cdot \mathbf{D} \nabla V_m - I_{\text{ion}}$$

where V_m is voltage across the cell membrane, C_m specific membrane capacitance, $\mathbf{D}$ a diffusion tensor and I_{ion} current flow though the cell membrane per unit area. This model has been described in detail in previous publications [25], [26].

We chose to use a model that simplifies both cell and tissue electrophysiology in order to reduce the computational load necessary to compute several seconds of VF in anatomically detailed geometry. We, therefore, calculated I_{ion} using the Fenton–Karma (FK) equations [13], [25] with the model parameters listed in [13, Table 1] to give the action potential duration (APD) and conduction velocity (CV) restitution of the

Beeler-Reuter model for ventricular cells. Although simplified, the FK model preserves the rapid upstroke velocity, overall shape and APD restitution of more complex cell models. With the chosen parameters, 3-D re-entry in this model readily breaks down into multiple wavelet re-entry as a result of dynamic heterogeneities in recovery that lead to regions of conduction block along the re-entrant wavefront [27], [28].

A simple explicit Euler scheme was used to solve the model equations with a time step (Δt) of 0.1 ms, and a space step (Δ) of 0.33 mm. We used methods described by Panfilov and Keener [29] to apply no-flux boundary conditions at each surface and to evaluate the diffusion tensor. We set C_m to 1 $\mu F \cdot cm^{-2}$ and set the longitudinal and transverse diffusion coefficients to $D_{\parallel} = 0.2$ mm$^2 \cdot$ ms^{-1} and $D_{\perp} = 0.05$ mm$^2 \cdot$ ms^{-1}, respectively. These values gave a plane wave speed of 0.64 ms^{-1} along fibers and 0.28 ms^{-1} across fibers. Changing Δt to 0.06, 0.08, 0.1, and 0.12 ms resulted in <1% change in plane wave speed with instability for $\Delta t > 0.14$ ms, and changing Δ to 0.3 mm and 0.4 mm resulted in a change in plane wave speed of <4% transverse and <2.5% longitudinal to fibers.

B. Anatomically Detailed Model of Canine Ventricles

We used the detailed canine ventricular anatomy and fiber orientation kindly provided by the University of Auckland (http://www.cmiss.org) [30]. We sampled the finite element description of both shape and fiber orientation on a regular Cartesian grid to give a ventricular geometry with 5 567 778 grid points [31], [32]. We have shown in a previous paper that the activation sequence following initiation of a normal beat by stimulating the endocardial surface was complete in 50 ms, and was quantitatively comparable with measured activation in canine ventricles [31].

C. Initiation of Re-Entry

To investigate the effect of VF originating in different locations, we initiated re-entry in the left ventricular (LV) free wall, right ventricular (RV) free wall, and septum by stimulating the base while maintaining a line of block running from base to apex for 120 ms. Fig. 1 shows this protocol for initiation in the LV free wall. In all three simulations we followed activity for 3 s after initiation.

D. Detection and Analysis of Filaments

We detected filaments from the intersection of $V_m = -20$ mV and $dV_m/dt = 0$ isosurfaces, and we identified voxels containing filaments using a method [25] based on that proposed by Fenton and Karma [13]. Filaments were identified from connected voxels at 1 ms intervals, and each filament allocated a unique number. The filament length, and the locations of each end (unless it was a closed ring) were also recorded. By comparing the overlap of filaments in two successive timesteps F_t and F_{t+1} we were able to identify the birth, death, bifurcation, amalgamation and continuation of filaments [25]. Filaments born in F_{t+1} did not overlap any filaments in F_t, whereas filaments that died in F_t did not overlap any filaments in F_{t+1}. A single filament in F_t bifurcated if it overlapped two or more filaments in F_{t+1}, and two or mor filaments in F_t amalgamated if they overlapped a single filament in F_{t+1}.
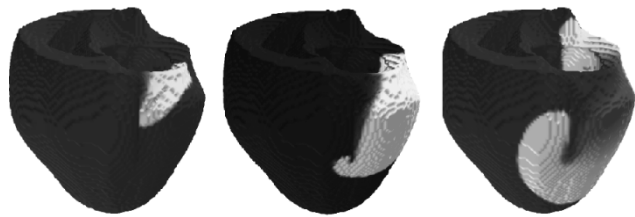

Fig. 1. Initiation of re-entry in the LV free wall. Voltage is shown as greyscale with depolarized regions white and repolarized regions grey. Frames show activity 40, 80, and 120 ms after stimulation in the basal LV free wall.

III. RESULTS

A. Effect of Initiation Site

Fig. 2 shows example time series of V_m recorded from the LV, RV, and septum together with snapshots of surface electrical activity and filaments following initiation of simulated re-entry in the LV free wall.

The first cycle of simulated re-entry produced an activation sequence that resulted in distinct action potentials in the LV free wall, RV free wall and septum. Following breakup of the initial re-entrant wave into simulated fibrillation, the number of filaments increased, the action potentials became shorter and their timing irregular.

Fig. 3 shows how the number of filaments increased during each simulation. Between 500 and 1000 ms after initiation in the LV free wall, the number of filaments increased at a rate of up to 70 s^{-1}. Following initiation in the thinner RV free wall and septum, the rate of breakup was about half of this value. All three simulations approached a steady-state beyond 1500 ms where the number of filaments in each simulation fluctuated around a mean value of 36.

We calculated cycle length (CL), diastolic interval (DI), and APD from points evenly distributed throughout the ventricles with a grid spacing of 3.3 mm (every tenth grid point). For initiation in the LV free wall the mean values of CL, DI, and APD were 101 ± 32 ms, 53 ± 20 ms, and 50 ± 25 ms. The mean CL, DI, and APD for initiation in the RV free wall and septum were not significantly different. Fig. 4 shows individual measurements of APD and the preceding DI for the initiation in the LV free wall, and compares these with the single-cell APD restitution curve for the FK model. We obtained an almost identical distribution of points for the other two simulations. Most points were shifted rightwards and downwards compared to the APD restitution curve, so that for a given DI the following APD was shorter than that predicted by the single-cell APD restitution curve.

Extracts from breakup graphs for all three simulations are shown in Fig. 5. The sustained multiplication of filaments began at around 500 ms, but was preceded in each case by transient break of the filament. Filament breakup close to the initiation site and then spread throughout the ventricles. The majority of filaments were descendants of the primary filament, although some filaments (shown in grey) were born separately and did not interact with the primary filament within
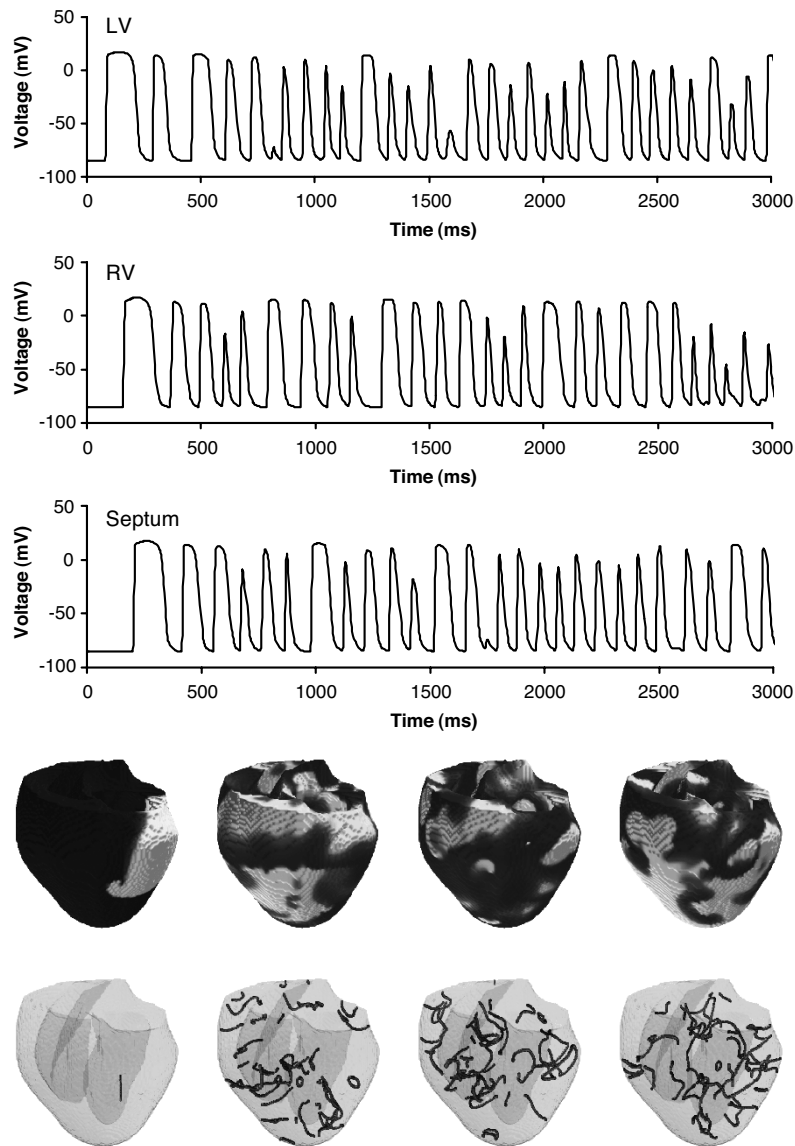
Fig. 2. Upper panels show time series of V_m recorded from the LV free wall (top), RV free wall (middle), and septum (bottom). Lower panels show distribution of V_m over the epicardial surface (top) and filaments (bottom) 80 ms, 1 s, 2 s, and 3 s after initiation in the LV free wall.
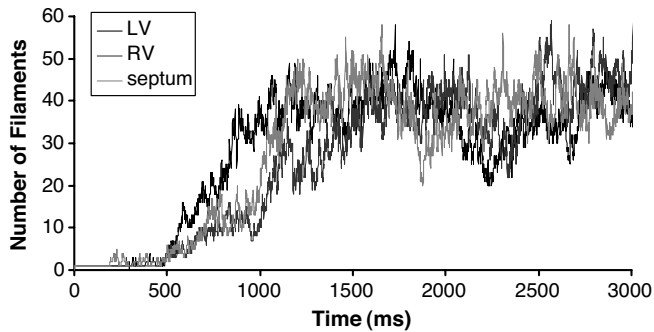
Fig. 3. Changes in the number of filaments following initiation of re-entry in the LV free wall (black), RV free wall (dark grey), and septum (light grey).

Fig. 4. Estimates of APD and preceding DI for activation following initiation of re-entry in the LV free wall (points) compared with single-cell APD restitution curve (line).

the time interval shown. The dominant mechanism for breakup following initiation in the LV free wall was a cascade of filament bifurcations. With initiation in the RV free wall and septum a cascade of filament bifurcations also occurred, but

many of these new filaments quickly died. We consider this issue further below.

(a) LV free wall

384 404 405 407 409 425 426 315   485 490 491 502 506 508 511 513 515 522 523 524 526 528

(b) RV free wall

280 281 283 464 475 505 506 516 517 518 519 521 522 523 525 527 528 529 530 531 532 533 534

(c) Septum

480 482 483 484 485 490 494 495 496 504 505 506 507 508 509 510 513 515 516 517 518 523 528

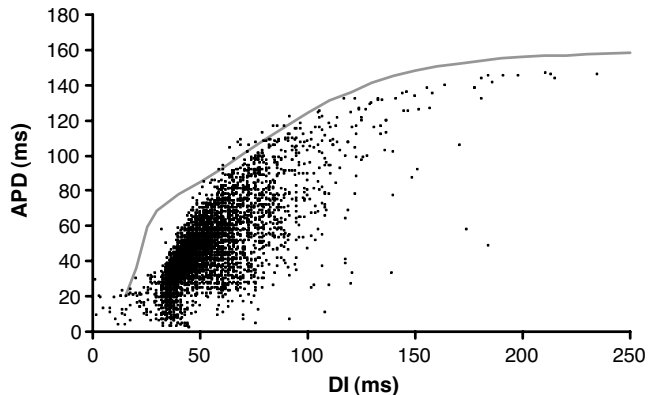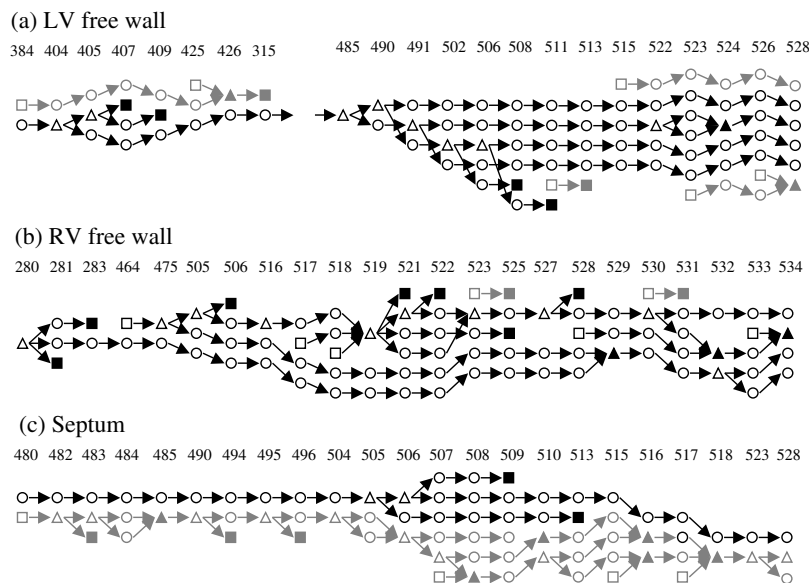Fig. 5. Filament graphs during the early part of each simulation. Numbers across the top of each graph are time from initiation in ms. Open squares denote filament births, and filled squares deaths. Open triangles denote filament bifurcation and filled triangles filament amalgamation. Open circles denote a continuation with no interaction. The primary filament and those connected to it are shown in black, other filaments in grey.
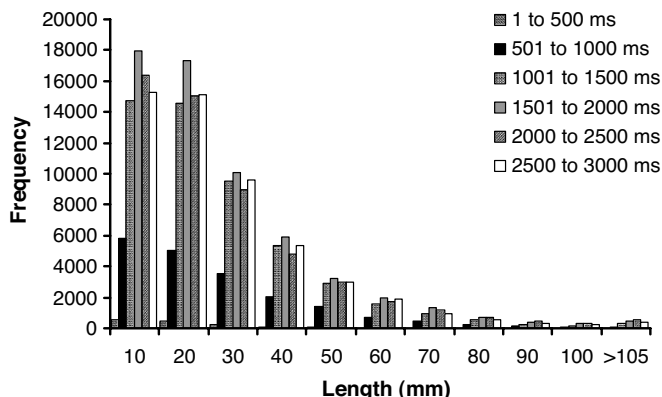
Fig. 6. Length of filaments during the 500 ms intervals shown. Y axis is the number of filaments with a particular length detected in the interval.
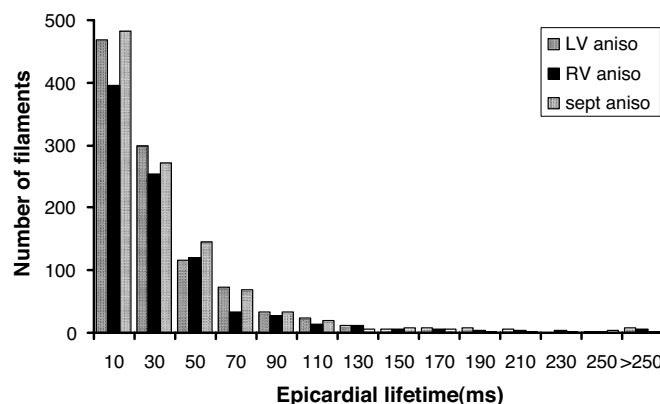
Fig. 7. Length of time for which ends of filaments were visible on the surface.

B. Filament Characteristics

The distribution of filament length is given in Fig. 6. In the canine ventricle geometry, the maximum thickness of the LV free wall is about 20 mm, and the maximum thickness of the RV free wall about 10 mm. The majority of filament lengths were close to these values, and the distribution of filament length did not change markedly during the simulation. Several longer filaments were detected, and these tended to lie intramurally.

We calculated the proportion of filaments with one or more ends touching the epicardial surface. There was no significant difference between the three simulations and the average overall was 65% with a standard deviation of 20%. The length of time that these filaments touched the surface is shown in Fig. 7, and only a tiny proportion of filaments were visible on the epicardial surface for more than one rotation period ($\approx$100 ms).

C. Filament Interactions

The total number of birth, death, bifurcation, and amalgamation events detected in each simulation is shown in Fig. 8(a). The

number of bifurcations was greater than the number of births, suggesting that in this model filament break occurs more frequently than wavebreak. The net gain in filaments (births + bifurcations − deaths − amalgamations) throughout each simulation was 34 for initiation in the LV free wall, 39 for initiation in the RV free wall, and 33 for initiation in the septum. These numbers were approximately two orders of magnitude lower than the number of filament creation (births + bifurcations) and destruction (deaths + amalgamations), showing that the majority of filaments either die or amalgamate with others. This extremely fine balance between filament creation and filament destruction is shown in more detail in Fig. 8(b)–(d). Even though more filaments are created between 200 and 600 ms following initiation in the septum than following initiation in the LV free wall, almost all of them die. Part of this sequence can be seen in Fig. 5, and this observation is consistent with the thicker LV free wall allowing more room for filament breakup than the thinner RV free wall and septum.
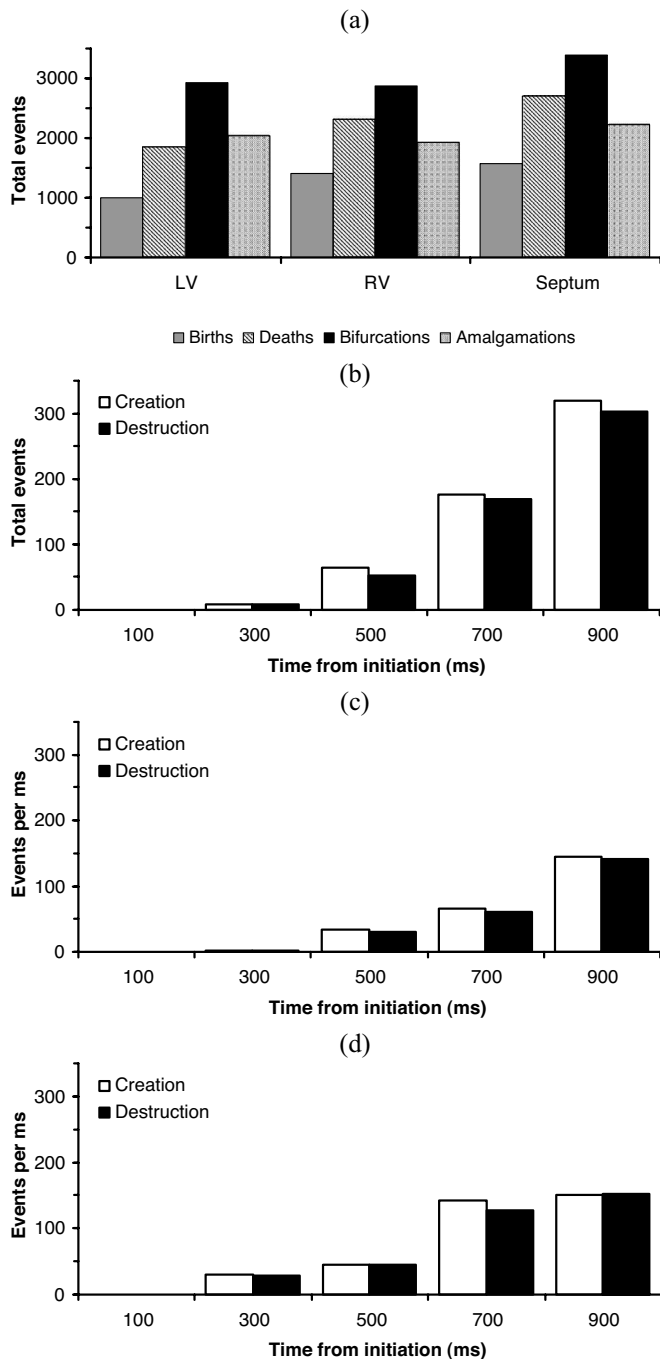
Fig. 8. (a) Overall number of births, deaths, bifurcations and amalgamations in each of the three simulations. Filament creation and destruction events during 200-ms epochs following initiation in (b) the LV free wall, (c) the RV free wall, and (d) the septum.

IV. DISCUSSION

A. Summary

This paper examines a computational model of re-entrant fibrillation in a detailed anatomical model of canine ventricles. We found that the site of initiation of re-entry had little effect on the mean number of filaments at steady-state, but the rate of increase of filaments during breakup was highest for initiation in the LV free wall, and lowest for initiation in the RV free wall. Although more than half of the filaments observed in this model touched the epicardial surface, most were visible for much less than one cycle of re-entry. Throughout breakup and sustained multiple wavelet re-entry the number of filaments created almost matched the number of filaments destroyed, and the balance between creation and destruction was finely poised.

B. Filament Detection and Breakup

In this study we located filaments by identifying points where isosurfaces of membrane voltage ($V_m = -20$ mV) and dV_m/dt crossed, and this approach has been used in other computational studies [11], [13]. As an alternative to calculating dV_m/dt, another approach identifies isolines or isosurfaces of a variable associated with recovery [33], [34]. Neither of these techniques are easy to use in experimental studies where variables associated with recovery cannot be directly measured and estimates of dV_m/dt may be very noisy. Other techniques based on phase analysis have, therefore, been developed to identify phase singularities in experimental data [4], and combined with information about chirality can be used to infer the structure of 3-D filaments [16].

Many different mechanisms may underlie breakup of re-entry, even in the simplified FK model [9]. The mechanism of breakup in our simulations appears to be related to steep APD restitution. Rotational anisotropy may have been important, although additional simulations in isotropic canine ventricle geometry also showed rapid breakup. It is possible that some aspects of filament behavior are affected by the mechanism of breakup because of differences in the head-tail interactions of re-entrant waves and the resulting wavebreaks. Our finding that the rate of filament increase was higher for initiation in the LV free wall compared to the RV free wall and septum indicates that wall thickness influences the rate of breakdown. Both of these issues remain as questions to be addressed by future projects.

C. Relation to Other Studies

The duration of re-entry on the epicardial surface has been shown to be short in experimental studies using in-situ pig ventricles [17], isolated hearts [4], [15], and ventricular wedge preparations [1], [19]. This is consistent with our model findings. We found that about 65% of about 36 filaments could intersect the epicardial surface of the ventricles during re-entrant VF in the canine heart, so our model predicts that about 20 phase singularities should be visible. This estimate is about four times higher than the number predicted from experimental observations in the sheep heart [4], which is roughly the same size. There are several possible reasons for this difference. First, our model is simplified and the limitations are discussed in detail below. Second, as discussed above several mechanisms of breakup may underlie the transition from re-entry to fibrillation, and could influence the number of filaments that form. Third, although more than half of the filaments in our model intersected the epicardial surface, most of them appeared for less than 10% of a rotation period and could possibly be missed in experimental recordings.

Our results are comparable with a previous computational study that used the Auckland canine geometry [24]. Although a different excitation model was used, the wavelength of re-entry in this study (average CL during VF × wavespeed) was 40 mm,

which is similar to the values of 64 mm longitudinal to fibers and 28 mm transverse to fibers obtained for our model, and the average number of filaments during steady-state was 38 compared with the average in our study of 36. There is also a agreement in the average length of filaments which was 30 mm in the present study and about 40 mm in the earlier study.

Although the length of time that filaments touch the epicardial surface can easily be measured from our model, the lifetime of filaments within the 3-D ventricular tissue themselves is harder to quantify. Fig. 7 shows that the many filaments are descended from the primary filament formed at initiation. Thus, although the brief manifestation of a filament on the surface could be described as a short-lived nonre-entrant wavebreak because it is both visible and active for less than one rotation, this feature could be associated with a filament that could trace its ancestry back through several cycles of re-entry.

D. Potential Implications

This study was not designed to investigate the effect of either VF mechanism or type of breakup on filament dynamics. However, this study does suggest that the location at which VF is initiated effects the rate of breakup, but not the eventual number or the dynamics of filaments. In our model the breakup of functional re-entry to multiple wavelet VF is rapid, and suggests that the number of filaments could increase from 1 to around 40 in less than 1 s during the early stages of VF. Breakup by other mechanisms [9] may result in different rates of filament multiplication. Nevertheless, experimental studies also suggest that the breakup of a single re-entrant wave into fibrillation can occur within a few cycles [35], [36], and this has implications for any therapy that attempts to provide an early intervention.

One of the main findings of this study is the suggestion that during breakup the balance of filament creation and filament destruction is could be extremely finely poised. Other large scale simulations of fibrillation in 3-D using other models suggest that this type of dynamic is not dependent on the model that we have used [11], [24], [33], and that it is likely to be a generic feature of complex 3-D re-entry. Several questions remain to be answered, including identifying which parameters are important in determining the balance of creation and destruction, and determining the influence of regional differences in both cell and tissue properties. Strategies that can alter this balance may be effective for antiarrhythmic and antifibrillatory therapy, and this balance may also be important in determining the success and failure of defibrillation shocks.

E. Study Limitations

Our model of action potential propagation is simplified at several levels. Although biophysically detailed models of cardiac cells and tissue have been developed [20], [21] they are computationally expensive to solve, and we chose to use an anisotropic monodomain model with excitation described by the FK equations in order to reduce the computational resources required to compute the evolution of re-entry over several seconds.

It is possible that filament behavior could be influenced by the use of different cell models, the more realistic boundary conditions that can be implemented with a bidomain tissue model, and allowing for the orthotropy of the fibrous sheet structure now believed to underlie ventricular tissue [30]. We also ignored the regional differences in action potential shape and duration that exist within normal ventricles, although in another study we have shown that these differences can pull apart re-entrant waves [37]. In addition we have simulated VF in normal tissue, yet re-entry and VF in the human heart are usually associated with pathology, especially regional ischaemia and infarction. Simulations of re-entry and VF that take into account these issues remain as important research challenges for the future.

Despite these simplifications, the APD and CV for action potential propagation in our model were within the range of values reported in experimental studies, the activation sequence of our simulated ventricles also matched with experimental observations [31], and the CL of re-entry during simulated VF was within the range of values reported experimentally [8].

REFERENCES

[1] M. Valderrabano, M. H. Lee, T. Ohara, A. C. Lai, M. C. Fishbein, S. F. Lin, H. S. Karagueuzian, and P. S. Chen, "Dynamics of intramural and transmural reentry during ventricular fibrillation in isolated swine ventricles," *Circ. Res.*, vol. 88, pp. 839–848, 2001.

[2] J. J. Lee, K. Kamjoo, D. Hough, C. Hwang, W. Fan, M. C. Fishbein, C. Bonometti, T. Ikeda, H. S. Karagueuzian, and P.-S. Chen, "Reentrant wave fronts in Wiggers' stage II ventricular fibrillation. Characteristics and mechanisms of termination and spontaneous regeneration," *Circ. Res.*, vol. 78, pp. 660–675, 1996.

[3] M. J. Janse, F. J. L. Van-Cappelle, H. Morsink, A. G. Kleber, F. Wilms-Schopman, R. Cardinal, C. N. D'Alnoncourt, and D. Durrer, "Flow of "injury" currents and patterns of excitation during early ventricular arrhythmias in acute regional myocardial ischaemia in isolated porcine and canine hearts. Evidence for two different arrhythmogenic mechanisms," *Circ. Res.*, vol. 47, pp. 151–165, 1980.

[4] R. A. Gray, A. M. Pertsov, and J. Jalife, "Spatial and temporal organization during cardiac fibrillation," *Nature*, vol. 392, pp. 75–78, 1998.

[5] R. A. Gray and J. Jalife, "Ventricular fibrillation and atrial fibrillation are two different beasts," *Chaos*, vol. 8, pp. 65–78, 1998.

[6] R. A. Gray, J. Jalife, A. V. Panfilov, W. T. Baxter, C. Cabo, J. M. Davidenko, and A. M. Pertsov, "Mechanisms of cardiac fibrillation," *Science*, vol. 270, pp. 1222–1223, 1995.

[7] A. V. Panfilov and A. M. Pertsov, "Ventricular fibrillation: Evolution of the multiple-wavelet hypothesis," *Philosophical Trans. Roy. Soc. Lond. Ser. A—Math. Physical and Eng. Sci.*, vol. 359, pp. 1315–1325, 2001.

[8] A. V. Zaitsev, O. Berenfeld, S. F. Mironov, J. Jalife, and A. M. Pertsov, "Distribution of excitation frequencies on the epicardial and endocardial surfaces of fibrillating ventricular wall of the sheep heart," *Circ. Res.*, vol. 86, pp. 408–417, 2000.

[9] F. H. Fenton, E. M. Cherry, H. M. Hastings, and S. J. Evans, "Multiple mechanisms of spiral wave breakup in a model of cardiac electrical activity," *Chaos*, vol. 12, pp. 852–892, 2002.

[10] V. N. Biktashev, A. V. Holden, and H. Zhang, "Tension of organizing filaments of scroll waves," *Philosophical Trans. Roy. Soc. Lond. Ser. A—Math. Physical and Eng. Sci.*, vol. 347, pp. 611–630, 1994.

[11] Z. L. Qu, K. Kil, F. G. Xie, A. Garfinkel, and J. N. Weiss, "Scroll wave dynamics in a three-dimensional cardiac tissue model: Roles of restitution, thickness, and fiber rotation," *Biophysical J.*, vol. 78, pp. 2761–2775, 2000.

[12] Z. L. Qu, J. N. Weiss, and A. Garfinkel, "Cardiac electrical restitution properties and stability of reentrant spiral waves: A simulation study," *Amer. J. Physiol.—Heart Circulatory Physiol.*, vol. 276, pp. H269–H283, 1999.

[13] F. Fenton and A. Karma, "Vortex dynamics in three-dimensional continuous myocardium with fiber rotation: Filament instability and fibrillation," *Chaos*, vol. 8, pp. 20–47, 1998.

[14] W. T. Baxter, S. F. Mironov, A. V. Zaitsev, J. Jalife, and A. M. Pertsov, "Visualizing excitation waves inside cardiac muscle using transillumination," *Biophysical J.*, vol. 80, pp. 516–530, 2001.

[15] J. Chen, R. Mandapati, O. Berenfeld, A. C. Skanes, and J. Jalife, "High-frequency periodic sources underlie ventricular fibrillation in the isolated rabbit heart," *Circ. Res.*, vol. 86, pp. 86–93, 2000.

[16] M.-A. Bray, S.-F. Lin, R. R. Aliev, B. J. Roth, and J. P. Wikswo, "Experimental and theoretical analysis of phase singularity dynamics in cardiac tissue," *J. Cardiovasc. Electrophysiol.*, vol. 12, pp. 716–722, 2001.

[17] J. M. Rogers, J. Huang, W. M. Smith, and R. E. Ideker, "Incidence, evolution, and spatial distribution of functional reentry during ventricular fibrillation in pigs," *Circ. Res.*, vol. 84, pp. 945–954, 1999.

[18] J. M. Rogers, J. Huang, R. W. Pedoto, R. G. Walker, W. M. Smith, and R. E. Ideker, "Fibrillation is more complex in the left ventricle than in the right ventricle," *J. Cardiovasc. Electrophysiol.*, vol. 11, pp. 1364–1371, 2000.

[19] M. H. Lee, Z. L. Qu, G. A. Fishbein, S. T. Lamp, E. H. Chang, T. Ohara, O. Voroshilovsky, J. R. Kil, A. R. Hamzei, N. C. Wang, S. F. Lin, J. N. Weiss, A. Garfinkel, H. S. Karagueuzian, and P. S. Chen, "Patterns of wave break during ventricular fibrillation in isolated swine right ventricle," *Amer. J. Physiol.—Heart Circulatory Physiol.*, vol. 281, pp. H253–H265, 2001.

[20] D. Noble and Y. Rudy, "Models of cardiac ventricular action potentials: Iterative interaction between experiment and simulation," *Philosophical Trans. Roy. Soc. Lond. Ser. A—Math. Physical and Eng. Sci.*, vol. 359, pp. 1127–1142, 2001.

[21] R. H. Clayton, "Computational models of normal and abnormal action potential propagation in cardiac tissue: Linking experimental and clinical cardiology," *Physiologic. Meas.*, vol. 22, pp. R15–R34, 2001.

[22] A. Garfinkel, Y. H. Kim, O. Voroshilovsky, Z. L. Qu, J. R. Kil, M. H. Lee, H. S. Karagueuzian, J. N. Weiss, and P. S. Chen, "Preventing ventricular fibrillation by flattening cardiac restitution," *Proc. Nat. Acad. Sci. USA*, vol. 97, pp. 6061–6066, 2000.

[23] V. N. Biktashev, A. V. Holden, S. F. Mironov, A. M. Pertsov, and A. V. Zaitsev, "Three-dimensional aspects of re-entry in experimental and numerical models of ventricular fibrillation," *Int. J. Bifurcation Chaos*, vol. 9, pp. 695–704, 1999.

[24] A. V. Panfilov, "Three-dimensional organization of electrical turbulence in the heart," *Phys. Rev. E*, vol. 59, pp. R6251–R6254, 1999.

[25] R. H. Clayton and A. V. Holden, "A method to quantify the dynamics and complexity of re-entry in computational models of ventricular fibrillation," *Phys. Med. Biol.*, vol. 47, pp. 225–238, 2002.

[26] ——, "Dynamics and interaction of filaments in a computational model of re-entrant ventricular fibrillation," *Phys. Med. Biol.*, vol. 47, pp. 1777–1792, 2002.

[27] M. Courtemanche, "Complex spiral wave dynamics in a spatially distributed ionic model of cardiac eletrical activity," *Chaos*, vol. 6, pp. 579–600, 1996.

[28] A. Karma, "Spiral breakup in model equations of action potential propagation in cardiac tissue," *Phys. Rev. Lett.*, vol. 71, pp. 1103–1107, 1993.

[29] A. V. Panfilov, "Re-entry in an anatomical model of the heart," *Chaos Solitons Fractals*, vol. 5, pp. 681–689, 1995.

[30] P. M. F. Nielsen, I. J. E. LeGrice, B. H. Smaill, and P. J. Hunter, "Mathematical model of geometry and fibrous structure of the heart," *Amer. J. Physiol. (Heart Circulatory Physiol.)*, vol. 29, pp. H1365–H1378, 1991.

[31] R. H. Clayton and A. V. Holden, "Computational framework for simulating the mechanisms and ECG of re-entrant ventricular fibrillation," *Physiologic. Meas.*, vol. 23, no. 4, pp. 707–726, 2002.

[32] ——, "Filament dynamics in a computational model of re-entrant fibrillation in anatomically detailed canine ventricular anatomy," in *Proc. 2nd Joint EMBS/BMES Conf.*, Houston, 2002, pp. 1417–1418.

[33] W.-J. Rappel, "Filament instability and rotational anisotropy: A numerical study using detailed cardiac models," *Chaos*, vol. 11, pp. 71–80, 2001.

[34] V. N. Biktashev and A. V. Holden, "Re-entrant waves and their elimination in a model of mammalian ventricular tissue," *Chaos*, vol. 8, no. 1, pp. 48–56, 1998.

[35] R. E. Ideker, G. J. Klein, L. Harrison, W. M. Smith, J. Kasell, K. A. Reimer, A. G. Wallace, and J. J. Gallagher, "The transition to ventricular fibrillation induced by reperfusion after acute regional ischaemia in the dog: A period of organized epicardial activation," *Circulation*, vol. 63, pp. 1371–1379, 1981.

[36] D. W. Frazier, P. D. Wolf, J. M. Wharton, A. S. L. Tang, W. M. Smith, and R. E. Ideker, "Stimulus induced critical point. Mechanism for electrical initiation of reentry in normal canine myocardium.," *J. Clin. Investigat.*, vol. 83, pp. 1039–1052, 1989.

[37] R. H. Clayton and A. V. Holden, "Effect of regional differences in cardiac cellular electrophysiology in the stability of ventricular arrhythmias: A computational study," *Phys. Med. Biol.*, vol. 48, pp. 95–111, 2003.

Richard H. Clayton received the B.Sc. degree in applied physics and electronics from the University of Durham, Durham, U.K., in 1986. He received the Ph.D. degree from the University of Newcastle upon Tyne, Newcastle upon Tyne, U.K., in 1990.

From 1990 until 1998, he worked on the analysis of ECG signals recorded during cardiac arrhythmias at the Freeman Hospital in Newcastle upon Tyne. An increasing interest in arrhythmia mechanisms led to a British Heart Foundation post at the University of Leeds, Leeds, U.K., where he developed computational models of re-entry and fibrillation. Since 2003, he has been with the Department of Computer Science at the University of Sheffield, Sheffield, U.K.

Arun V. Holden received the B.A. degree in animal physiology from the University of Oxford, Oxford, U.K., in 1968, and the Ph.D. degree in physiology from the University of Alberta, Edmonton, AB, Canada, in 1971.

He is the Chair of Computational Biology at the University of Leeds, Leeds, U.K. He has been based in Leeds since 1971. His research interests are focussed around integrative computational biology, and nonlinear dynamics.

Dr. Holden is on the editorial boards of several nonlinear science journals (*International Journal of Bifurcation and Chaos*, and *Chaos, Solitons and Fractals*) and is an editor of the Wiley Series in Nonlinear Science.